





A Collaborative Filtering Approach Toward Plug-and-Play Myoelectric Robot Control

Jun-ichiro Furukawa , *Member, IEEE*, Shinya Chiyohara , Tatsuya Teramae ,
Asuka Takai , and Jun Morimoto, *Member, IEEE*

Abstract—Previous works in the literature have claimed that the characteristics of electromyography (EMG) signals depend on each person, and thus, EMG interfaces need to be carefully calibrated for each user in myoelectric control. In this study, we show that the EMG interface used to estimate the joint torques of a user can be constructed simply by incorporating other users' data without typical calibration process. To achieve this plug-and-play capability, we introduce the concept of collaborative filtering to estimate the joint torque of a novel user by exploiting the preidentified relationships between motion-body features, including EMG signals, and the joint torques of other users. To validate our proposed approach, we compare the performance of estimating joint torque by the proposed method with that by conventional linear regression models as a baseline. We considered the following two baseline methods. *Linear-own*: The parameters of the linear model are calibrated for each subject from his/her own training data. *Linear-others*: The parameters of the linear model are calibrated with the other users' data in which the novel user's data are not included. As a result, the estimated joint torques from our proposed approach reveal a better estimation performance than those from the baseline approaches. Furthermore, we also successfully demonstrate online myoelectric control of an upper limb exoskeleton robot with an attached mannequin arm.

Index Terms—Calibration process reduction, collaborative filtering, electromyography (EMG), motion estimation, myoelectric control.

I. INTRODUCTION

MYOELECTRIC interfaces have great potential to provide an intuitive way of controlling external devices for human users. In particular, intuitive interfaces are desirable for prosthetic devices or exoskeleton assistive robots [1], [2] to allow users to control them as a part of their own body.

To build a myoelectric interface, the measured muscle activities must be converted to control the commands for external devices. Previous studies have mainly adopted either classification methods or regression approaches. In the former, such movement classes as hand postures were predicted from electromyographies (EMGs) [3], [4]. In the latter, the interfaces were trained to estimate such user control commands as joint torques from EMG signals [5]–[8]. For both approaches, calibration procedures are needed to determine the parameters for estimating the user-intended output from EMG signals. Moreover, these calibrations are usually required for each subject and each experiment, since the relationships between the EMGs and the user-intended control outputs tend to be varied. Requiring such a cumbersome procedure inhibits the potential distribution of useful myoelectric interfaces. As a matter of fact, the calibration procedure requires tens of minutes to learn one model [9], perhaps even more for nonexperts. Minimizing the calibration process is a challenge that must be met for assistive devices [10].

In this study, we construct an EMG interface that estimates a user's joint torques simply with the data of other users. In other words, our proposed method requires no time-consuming calibration process for each new user. This plug-and-play EMG interface can be achieved by carefully taking human muscle-skeletal properties into account.

- 1) The amplitudes of EMG signals are observed according to muscle tensions [11], [12].
- 2) This relationship between EMG signals and muscle tensions depends on muscle mass [13].
- 3) The relationship between muscle tension and joint torque depends on the limb length and the joint angle.

From the aforementioned three properties, we found that the relationship between joint torques and motion-body features can be generalized among different users, where the motion-body features are composed of EMG signals, joint angles, body weight, and limb lengths. In our approach, this generalization

Manuscript received November 10, 2020; revised March 20, 2021 and May 24, 2021; accepted June 11, 2021. Date of publication August 5, 2021; date of current version September 15, 2021. This work was supported in part by "Research and development of technology for enhancing functional recovery of elderly and disabled people based on noninvasive brain imaging and robotic assistive devices," which is commissioned research of the National Institute of Information and Communications Technology (NICT), Japan, in part by JSPS KAKENHI under Grant JP18K18135, Grant 16H06565, and Grant JP21K17836, and in part by JST, ACT-I under Grant JPMJPR18UQ, Japan. This article was recommended by Associate Editor X. Hu. (*Corresponding author: Jun-ichiro Furukawa.*)

Jun-ichiro Furukawa is with the Man-Machine Collaboration Research Team, Guardian Robot Project, RIKEN Information R&D and Strategy Headquarters, Kyoto 619-0288, Japan, and also with the Advanced Telecommunications Research Institute International (ATR), Kyoto 619-0288, Japan (e-mail: junichiro.furukawa@riken.jp).

Shinya Chiyohara and Tatsuya Teramae are with the Advanced Telecommunications Research Institute International (ATR), Kyoto 619-0288, Japan (e-mail: s.chiyohara@atr.jp; t-teramae@atr.jp).

Asuka Takai is with the Advanced Telecommunications Research Institute International (ATR), Kyoto 619-0288, Japan, and also with the Graduate School of Engineering, Osaka City University, Osaka 558-8585, Japan (e-mail: atakai@atr.jp).

Jun Morimoto is with the Man-Machine Collaboration Research Team, Guardian Robot Project, RIKEN Information R&D and Strategy Headquarters, Kyoto 619-0288, Japan, with the Advanced Telecommunications Research Institute International (ATR), Kyoto 619-0288, Japan, and also with the Graduate School of Informatics, Kyoto University, Kyoto 606-8501, Japan (e-mail: xmorimo@atr.jp).

Color versions of one or more figures in this article are available at <https://doi.org/10.1109/THMS.2021.3098115>.

Digital Object Identifier 10.1109/THMS.2021.3098115

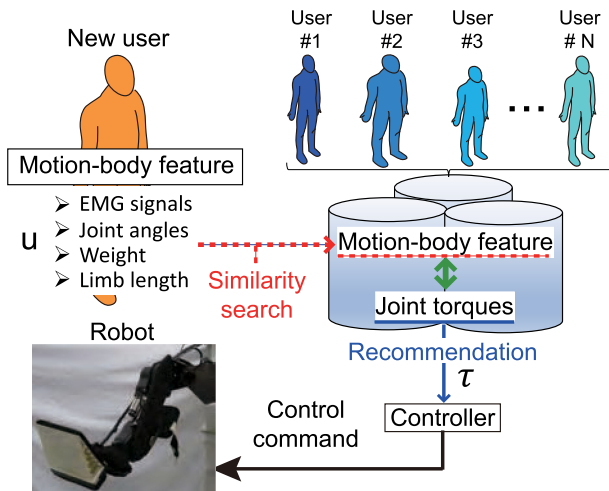


Fig. 1. Schematic diagram of the proposed collaborative filtering approach to constructing a plug-and-play myoelectric interface. Measured motion-body feature (EMG, joint angle, body weight, and limb length) queries correspond to joint torque for controlling external devices without a calibration process.

property is applied to a collaborative filtering framework often used for recommendation systems [14].

Fig. 1 shows a schematic diagram of the proposed approach. We first find the relationships between motion-body features and the corresponding joint torques, where the joint torque patterns are derived from inverse dynamics models. In other words, we annotate the motion-body features with the joint torques. From newly observed EMG signals, joint angles, body weight, and limb length information of a novel user, we obtain the corresponding joint torques using the collaborative filtering method.

This article offers the following contributions.

- 1) The relationship between joint torques and motion-body features is generalized among different users, where motion-body features are composed of EMG signals, joint angles, body weight, and limb length.
- 2) The extracted relationships between the joint torques and the motion-body features from other users are found to be more useful than the results of a standard linear regression model in which the parameters are calibrated with the user's own data.
- 3) The generalization property is successfully applied to achieve plug-and-play myoelectric control of a real robot using collaborative filtering.

In our preliminary study [15], we reported that the collaborative filtering approach is potentially useful for estimating joint torques from EMG signals (not from motion-body features). In experiments with a limited number of subjects, we showed that our proposed method's torque estimation performance (without a calibration process) was comparable with that of the standard linear regression model that requires calibration.

On the other hand, in this study, by newly taking the biomechanical information of human users into account, we show that our collaborative filtering approach outperforms the standard methods through comprehensive experiments using ten subjects. Furthermore, we now demonstrate that the data collected in

single joint movements can be used to estimate the joint torques of multijoint arm movements.

The rest of this article is organized as follows. Section II describes related works. In Section III, we introduce our approach to constructing a plug-and-play EMG interface. Section IV describes our experimental setups, and Section V shows our experimental results. We compared the joint torque estimation performances with baseline standard linear regression models and show online upper limb exoskeleton robot control performances. In Section VI, we discuss how each motion feature element contributed to the torque estimation performance. Finally, Section VII concludes this article.

II. RELATED WORKS

Multuser adaptation methods for myoelectric interfaces have been explored in the previous literature to reduce the burden of calibration processes. Although standard EMG-based interfaces need to be calibrated for each user, the parameters acquired from others can at least be useful for initializing a motion classifier [16], decomposing EMG spike profiles for gesture recognition [17], and deriving a style-content separation model for one-shot classifier learning [18]. However, the aforementioned models still require the data of novel users, and the output of their interfaces is discrete motion labels rather than a continuous output, which is desirable for assistive control.

Using regression to derive the parameters of myoelectric interfaces is a standard approach for continuous EMG-based control. In this approach, the joint torque or muscle tension values used to control external devices are estimated from EMG signals and motion data [19]. Due to its simplicity, using a linear model for the interface has been a popular regression approach [5], [20]–[23]. However, capturing complicated biomechanical properties by simply using linear models limits the performance of estimating the user's movement intentions.

On the other hand, muscle tension models [24] have been proposed that range from simple to quite complex models, including one previous model [25] that required 50 parameters to describe a simple joint motion. Although complex models are expected to have high expressive capability, model learning becomes difficult due to the requirement of large-scale data for calibrating a great number of parameters for each user [26].

To the best of our knowledge, this paper describes the first study of a multuser data-driven approach to constructing a myoelectric interface that does not require a calibration process for novel users.

III. METHOD

A. Data Collection and Annotation

We first stored the motion-body feature dataset \mathbf{u}^{DB} of multiple subjects into a database (see Fig. 1).

1) *Data Collection*: The motion-body feature is represented as follows:

$$\mathbf{u}'(t) = [\mathbf{e}^\top(t), \Theta^\top(t), W, L]^\top \quad (1)$$

where \mathbf{e} is the EMG vector, Θ is the joint angle vector, W denotes the body weight information, and L represents the limb length. Here, the N -channel EMG signal vector is represented as $\mathbf{e}(t) = [e^1(t), e^2(t), \dots, e^N(t)]$. Each element of the EMG vector $e(t)$ is derived as a moving summation of a processed EMG signal for a fixed period

$$e^i(t) = \sum_{n=t-l}^t z^i(n) \Delta t. \quad (2)$$

This is because the EMG signals are activated a few milliseconds prior to the actual limb movements [8]. We take a time delay between EMG signal observation and actual movement generation into account by introducing latency l . Furthermore, in order to find similarity to other users' data, the i th processed EMG signals s^i are normalized as follows:

$$z^i(n) = \frac{s^i(n) - s_{\text{rest}}^i}{s_{\text{mvc}}^i} \quad (3)$$

where the processed EMG signal s^i is derived as a full-wave rectified and low-pass filtered value of the i th raw EMG measurement with cutoff frequency of 8 Hz. Here, s_{rest}^i indicates the resting value and s_{mvc}^i denotes the maximum voluntary contraction (MVC) output.

To evaluate the distance among motion-body features $\mathbf{u}'(t)$ in (1), we normalized each component of the feature vector. Concretely, we normalized it as

$$\mathbf{u}(t) = (\mathbf{u}'(t) - \mathbf{U}'_{\min}) \oslash (\mathbf{U}'_{\max} - \mathbf{U}'_{\min}) \quad (4)$$

where the elements of the vectors \mathbf{U}'_{\min} and \mathbf{U}'_{\max} are minimum and maximum of each component of the motion-body feature data, respectively. These vectors were detected from all of the other users' data. Here, the notation \oslash denotes element-wise (Hadamard) division.

2) *Data Annotation*: We then annotated the stored data with the joint torque values. Following previous studies [6], [8], [19], the joint torque τ^{DB} was computed from the inverse dynamics of a subject's limb

$$\tau^{DB} = \mathbf{M}(\Theta)\ddot{\Theta} + \mathbf{h}(\Theta, \dot{\Theta}) + \mathbf{g}(\Theta) \quad (5)$$

where Θ represents the joint angles, $\mathbf{M}(\Theta)$ is the inertia matrix, $\mathbf{h}(\Theta, \dot{\Theta})$ denotes the centripetal Coriolis and viscosity, and $\mathbf{g}(\Theta)$ is the gravity term. The subject's body parameters used to calculate the inverse dynamics, such as each link weight of the limb and center of each link mass, were computed based on a previous formulation [27] after measuring the subject's body weight and limb length.

B. Collaborative Filtering

Collaborative filtering methods have been widely used to estimate a novel user's purchasing preferences from other users' product selection records by finding similarity between the novel user and other users' profiles [28]. In order to implement this concept of collaborative filtering, in this study, we adopt one of the most popular implementations using k -nearest neighbor (k -NN) [29], [30]. By using this approach, joint torques of the novel user can be estimated by measuring the similarity between

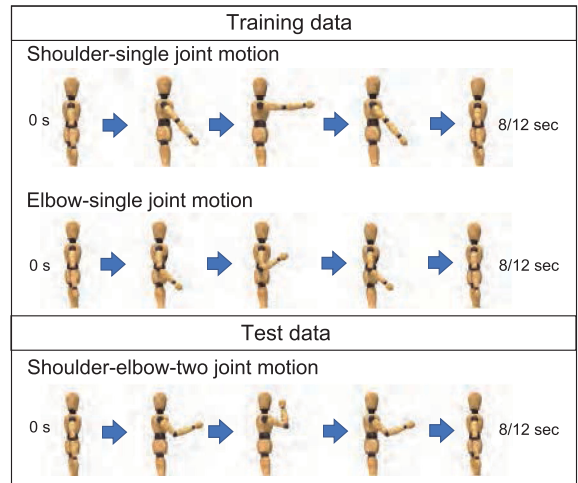


Fig. 2. We measured three types of motions: shoulder and elbow single-joint motions as training data, i.e., stored in database, and shoulder–elbow multijoint motion as test data, i.e., query.

the novel user's motion-body feature data and the k -nearest other user's data (see Fig. 1).

With the k -NN, the j th joint torque of a novel user $\tau^j(t)$ is estimated as

$$\tau^j(t) = \frac{\sum_{i=1}^k \frac{\tau_i^{DBj}}{D(\mathbf{u}(t), \mathbf{u}_i^{DBj})}}{\sum_{i=1}^k \frac{1}{D(\mathbf{u}(t), \mathbf{u}_i^{DBj})}} \quad (6)$$

where $D(\mathbf{u}(t), \mathbf{u}_i^{DBj})$ represents the similarity between the motion-body feature of the novel user $\mathbf{u}(t)$ and the i th nearest that of the database \mathbf{u}_i^{DBj} . In our experiments, we use the Euclidean norm to calculate the similarity as $D(\mathbf{u}(t), \mathbf{u}_i^{DBj}) = \|\mathbf{u}(t) - \mathbf{u}_i^{DBj}\|$.

IV. EXPERIMENTAL SETUP

A. Experimental Design

In order to validate our proposed approach, we considered the following three types of upper limb motions: 1) shoulder single-joint motion, 2) elbow single-joint motion, and 3) shoulder–elbow multijoint motion. From the perspective of reducing the calibration process, this study focuses on evaluating the case where the motion tasks are different between the training and the test phases. Concretely, the single-joint motions in 1) and 2) were stored in the database as training data and the multijoint motion 3) was used only to evaluate the joint torque estimation performance as test data (see Fig. 2).

We asked subjects to carry out three types of motions under the following four conditions.

- 1) Cond. 1: Slow speed (12 s/motion) with no-load condition.
- 2) Cond. 2: Slow speed (12 s/motion) with load (female: 0.5 kg, male: 1.0 kg) condition.
- 3) Cond. 3: Medium speed (8 s/motion) with no-load condition.

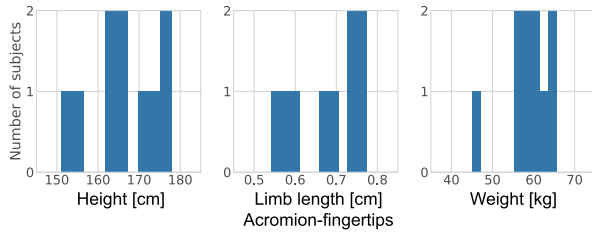


Fig. 3. Subject characteristics. Body features are widely different among subjects.

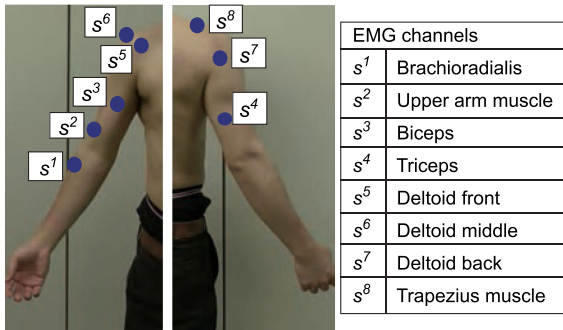


Fig. 4. EMG electrode locations on upper limb. EMG sensors for measuring muscle activities related to each joint movement were placed around anatomically plausible locations.

- 4) Cond. 4: Medium speed (8 s/motion) with load (female: 0.5 kg, male: 1.0 kg) condition.

Subjects were asked to complete the target motion within 12 and 8 s in the slow- and medium-speed conditions, respectively.

We measured joint motion of ten healthy right-handed subjects [four male and six female subjects, age: 21 to 33 (mean 26), height: 151 to 178 cm (mean 166 cm), weight: 45 to 66 kg (mean 59 kg)] who gave informed consent. Only healthy subjects participated in this experiment, and Fig. 3 shows the histogram of subject characteristics. All experiments were approved by the ethics committee of the Advanced Telecommunications Research Institute International, Kyoto, Japan, and were conducted according to the Declaration of Helsinki. For each subject and each motion type, we asked subjects to generate the movement four times. In total, 320 single-joint motions were measured and stored in the database. On the other hand, 160 multijoint motions were measured for the test data. In our evaluation, one subject was selected as a novel user from among the ten subjects, and the remaining nine subjects' data were used to estimate the joint torque. Then, the process was repeated nine more times with each subject acting one time as the novel user.

B. Data Collection and Annotation

We simultaneously recorded the EMG signals and joint angle trajectories when subjects generated target limb movements. Body weight and upper limb length were also measured for each subject.

Fig. 4 shows the EMG channel locations used to measure muscle activities from the right upper limb using eight EMG sensors. We used Ag/AgCl bipolar surface EMG electrodes and derived the processed EMG signals from the brachioradialis

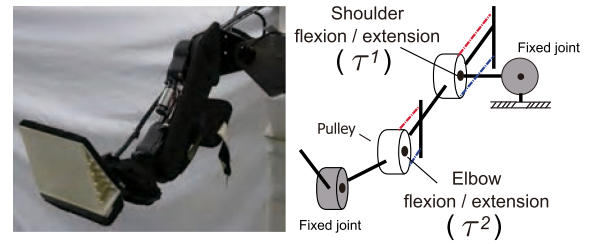


Fig. 5. Upper limb exoskeleton robot. Shoulder flexion/extension and elbow flexion/extension are actuated by pneumatic-electric hybrid actuators. In this study, shoulder abduction/adduction and wrist flexion/extension joints were not used, i.e., they were fixed.

(s^1), the upper arm muscle (s^2), the biceps (s^3), the triceps (s^4), the deltoid front (s^5), the deltoid middle (s^6), the deltoid back (s^7), and the trapezius muscle (s^8). To obtain MVCs, we asked subjects to generate maximum muscle forces while our physiotherapist gave resistance against the subject's upper limb movements. In order to measure the joint angle trajectories and limb length, we utilized a motion capture system (OptiTrack Japan, Ltd). The data measured from the motion capture system often include sensor noises and missing data. Therefore, we derived the joint angle trajectories and limb length from the marker data using the probabilistic inference [31] to deal with them. As for acquiring the body weight information, we used a force plate system.

We sampled the amplified EMG with a sampling rate of 1 kHz, i.e., the sampling period was $\Delta t = 1$ ms in (2). For the joint angles, we measured the marker position with a sampling rate of 125 Hz. After the preprocessing described in (2) and (3), EMG signals were down-sampled to match the size of the motion capture data.

We also derived joint torque sequences from the inverse dynamics model of a subject's limb to annotate the motion-body feature data. In the load conditions, the load weight was added to the mass of the hand in the inverse dynamics calculation.

C. Collaborative Filtering

In our collaborative filtering approach, the distance D in (6) is calculated by Euclidean norm. The number of neighboring data k of k -NN in (6) and the time period for summing the EMG observations l in (2) were set through cross validation as described in Appendix A. Note that we did not conduct any calibration procedure for a novel subject to estimate the joint torque when we used our collaborative filtering approach. U'_{\min} and U'_{\max} in (4) used for the normalization were determined only from the single-joint motion data, i.e., training data.

D. Upper Limb Exoskeleton Robot

In our real robot experiment, the estimated joint torques of the novel user are used to control multiple joints of our upper limb exoskeleton robot: elbow flexion/extension and shoulder flexion/extension (see Fig. 5). The details of the mechanical design and the torque-based control method of the exoskeleton robot were introduced in our previous studies [6], [32]. In order to generate joint motions with the exoskeleton robot using the

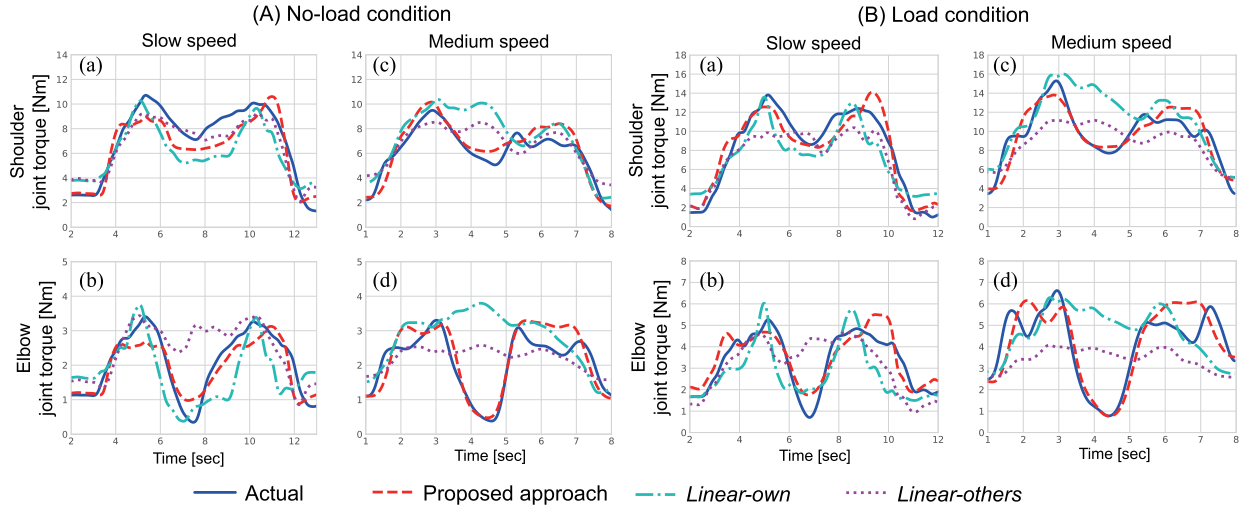


Fig. 6. Estimated joint torque profiles during multijoint upper limb movement. (A) No-load condition. (B) Load condition. (a) and (b) Shoulder joint movements. (c) and (d) Elbow joint movements. Solid blue line shows actual joint torques derived from inverse dynamics. Dashed red line shows estimated joint torques by our proposed approach. Dash-dotted cyan line shows estimated joint torques by *Linear-own*. Dotted purple line shows estimated joint torques by *Linear-others*. The proposed approach shows better estimation performance than standard methods. Each torque profile in this figure was postprocessed with a second-order Butterworth lowpass filter with cutoff frequency of 1.6 Hz. Note that this cutoff is used only for better visualization, while the actual cutoff is 8 Hz.

estimated torque, a mannequin arm was attached to the robot so that the dynamical properties would come closer to the subject's data.

V. RESULTS

In order to evaluate the torque estimation performance of our proposed approach, we compared it with standard linear regression models [5], [33], [34]. Concretely, we considered the following two baseline torque estimation methods:

- 1) *Linear-own*: The parameters of the linear model were calibrated for each novel user from their own training data.
- 2) *Linear-others*: The parameters of the linear model were calibrated with the other users' data in which the novel user's data were not included.

Detailed implementations are described in Appendix B. Note that our proposed approach also does not use any of the novel user's own data.

A. Torque Estimation Performance

We compared the joint torque estimation performance of the proposed approach with *Linear-own* and *Linear-others* using test data acquired from the multi-joint motions. To calibrate the parameters of *Linear-own* and *Linear-other* methods, we used only the single-joint motions as depicted in Fig. 2. Then, the multijoint motion data were used for performance evaluations. As an example of torque estimation results, Fig. 6 shows the torque estimation performances of our proposed approach, *Linear-own*, and *Linear-others* for one of the ten subjects: Fig. 6(A) shows results with the no-load condition. Fig. 6(B) shows results with the load condition. The top four panels represent shoulder joint movements and the bottom four panels represent elbow joint movements. Each panel shows the results with either slow- or medium-speed condition. The actual torque profiles were

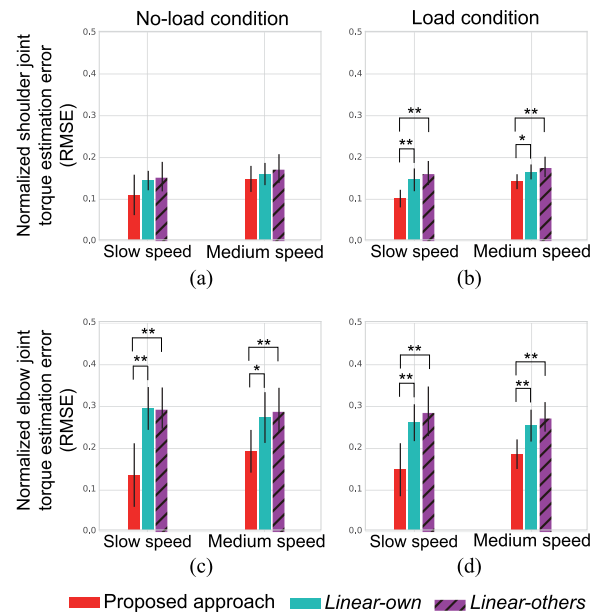


Fig. 7. Comparison between joint torque estimation performances (RMSEs) of the proposed and standard linear regression models in multijoint motion. (a) and (b) *No-load* condition, and (c) and (d) *Load* condition results. (a) and (c) Shoulder joint torque estimation performances. (b) and (d) Elbow joint estimation performances. *Slow-speed* condition: 12 s/motion and *medium-speed* condition: 8 s/motion. In all conditions, the proposed approach outperformed two baseline linear regression methods (*Linear-own* and *Linear-others*) in terms of averaged torque prediction error. We further applied a paired *t*-test adjusted by Bonferroni correction to torque estimation errors of *Linear-own* and *Linear-others* with reference to the proposed approach. We found statistically significant differences between the proposed approach and baseline methods except for the case in panel (a) (* : $p < 0.05$, ** : $p < 0.01$).

derived from the inverse dynamics of a novel user's limb with the actual joint trajectories.

Fig. 7 shows the torque estimation errors averaged over all ten subjects for the test data. We plotted normalized torque

TABLE I
STATISTICAL ANALYSIS WITH REFERENCE TO PROPOSED APPROACH

Speed	Statistics	<i>Linear-own</i>	<i>Linear-others</i>
(a) Slow		n.s	n.s
(a) Medium		n.s	n.s
(b) Slow	p	0.00066	0.00044
	$t(9)$	5.6	5.9
	CI	[0.099 – 0.22]	[0.11 – 0.22]
	Cohen's d (effect size)	2.6	2.8
(b) Medium	p	0.038	0.0011
	$t(9)$	2.9	5.3
	CI	[0.021 – 0.14]	[0.060 – 0.14]
	Cohen's d	1.3	2.5
(c) Slow	p	< 0.0001	0.00021
	$t(9)$	8.0	6.5
	CI	[0.033 – 0.057]	[0.043 – 0.083]
	Cohen's d	3.8	3.1
(c) Medium	p	0.030	< 0.0001
	$t(9)$	3.0	7.82
	CI	[0.0070 – 0.040]	[0.027 – 0.047]
	Cohen's d	1.4	3.7
(d) Slow	p	0.00011	0.0049
	$t(9)$	7.1	5.9
	CI	[0.079 – 0.15]	[0.090 – 0.19]
	Cohen's d	3.8	2.8
(d) Medium	p	0.0063	0.0032
	$t(9)$	4.0	6.2
	CI	[0.032 – 0.11]	[0.060 – 0.12]
	Cohen's d	1.9	2.9

estimation errors where the errors were divided by the maximum value of the actual joint torques. As shown in Fig. 7, in all of the conditions, our proposed approach outperformed the two baseline linear regression methods (*Linear-own* and *Linear-others*) in terms of averaged torque prediction error. We further applied a paired t -test adjusted by Bonferroni correction to the torque estimation errors of *Linear-own* and *Linear-others* with reference to the proposed approach. Table I shows the results of statistical analysis. Blocks indexed with (a)–(d) correspond to (a)–(d) in Fig. 7, and we found statistically significant differences between the estimation performances of the proposed method and the baseline models in most cases. On the other hand, we found no significant differences between the proposed approach and baseline methods for the case of shoulder joint torque estimation with *no-load* condition. For this particular case, the normalized errors are smaller than in other cases. This result indicates that the relationship between the joint torques and motion-body features are relatively simple in the flexion-extension shoulder joint movements without any load, and the relationship can be captured relatively well not only by the proposed approach but also by the simple linear models.

We compared the normalized RMSE values of the proposed approach with those of the baseline methods under each of the eight conditions shown in Fig. 7. Then, we counted the actual number of subjects whose performances were higher, i.e., a smaller RMSE, with the proposed approach than with the baseline methods. The averaged counts were 8.8 out of 10 against *Linear-own* and 9.3 out of 10 against *Linear-others*.

Our proposed collaborative filtering approach outperformed the *Linear-own* model, which requires a calibration process. In other words, by properly applying the data acquired from other users, we can achieve a better myoelectric interface than one requiring the user's own data. This capability allows us to develop plug-and-play myoelectric interfaces.

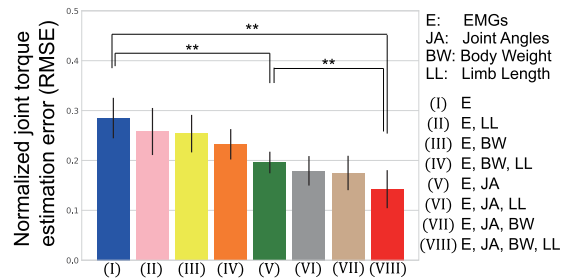


Fig. 8. Comparison among joint torque estimation performances (RMSEs) using the proposed method with different motion-body feature sets. We investigated how each element contributed to improving the torque estimation performance. Consequently, each element seemed to provide a nearly equivalent contribution. We applied the Wilcoxon signed-rank test adjusted by Bonferroni correction to the estimation performances of three different features (** : $p < 0.0001$).

The average computational time needed to estimate the joint torque using the proposed collaborative filtering method was about 1.4 ms on a computer equipped with Intel(R) Xeon(R) CPU E5-1650 v4 at 3.6 GHz. This result indicates that we can apply our approach to real-time control.

B. Generalization Performance Among Different Users

Since we aimed to minimize the calibration process for a novel user to generate novel movements, we conducted different motion tasks between the training and the test phases in our experiments. On the other hand, here, to highlight the generalization performance among different users, we gave attention to the estimation performances for the single-joint motions. Concretely, we used single-joint motion data both for training and test phases. Because our goal is to see the generalization performance among different users, the *Linear-own* model is out of our focus. Thus, we compared our proposed method with *Linear-others*. The normalized and averaged torque estimation errors over the load/no-load conditions and shoulder/elbow joints were 0.17 for our model and 0.26 for the *Linear-others* model. These results clearly show the effectiveness of our approach of using other users' data for a novel user.

C. Contribution to Estimation Performance of Each Element in Feature Vector

In this study, in addition to EMG signals, we took joint angle, body weight, and limb length into account as the elements of the motion-body feature. Here, we investigate how each element contributed to improvement of joint torque estimation performance. Fig. 8 shows the averaged torque estimation performances of the proposed approach over all experimental conditions with different motion-body features. We plotted normalized torque estimation errors as in Fig. 7. We found that each element seemed to provide a nearly equivalent contribution to improving the torque estimation performance. Here, we highlighted the effects of the “joint angle” element and the combined “body weight + limb length” element. We applied the Wilcoxon signed-rank test adjusted by Bonferroni correction to the joint torque estimation performances by the proposed approach among cases with the three different features: $\mathbf{u}' = [\mathbf{e}^T(t)]^T$,

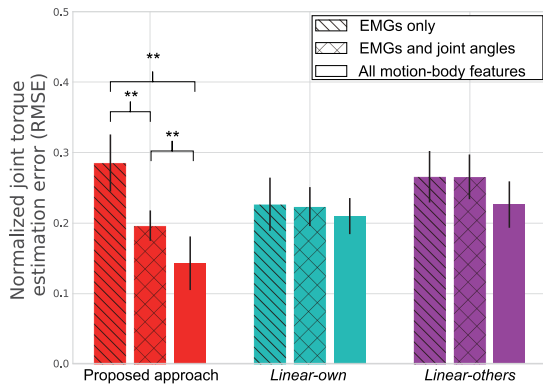


Fig. 9. Comparison among joint torque estimation performances (RMSEs) of different motion body features: “EMGs only,” “EMGs and joint angles,” and all-motion body elements in proposed, *Linear-own*, and *Linear-others*. We applied the Wilcoxon signed-rank test adjusted by Bonferroni correction to estimation performances of three different features in each method. We found significant difference between “EMGs only” and “EMGs and joint angles”: $p < 0.0001$, between “EMGs and joint angles” and “All motion-body features”: $p < 0.0001$, and between “EMGs only” and all motion-body features: $p < 0.0001$ in the proposed approach. On the other hand, we did not find significant differences in *Linear-own* and *Linear-others* methods.

$\mathbf{u}' = [\mathbf{e}^\top(t), \Theta^\top(t)]^\top$, and $\mathbf{u} = [\mathbf{e}^\top(t), \Theta^\top(t), W, L]^\top$. As a result, we found significant differences among them, and the estimation performance gradually improved as each element was included.

Fig. 9 shows a comparison of the averaged torque estimation performances among the proposed method and baseline linear regression models with different motion-body features. Specifically, we investigated the performances when using EMGs only, EMGs and joint angles, and all motion-body features. We applied the Wilcoxon signed-rank test adjusted by Bonferroni correction to the estimation performances of three different features in each method. We found significant differences among the three different features in our proposed approach, but not in the *Linear-own* and *Linear-others* methods. Although *Linear-own* showed better performance than the proposed method when the EMGs only feature was used, *Linear-own* needs the user’s own data while ours does not. Results indicate that the proposed method can take advantage of incorporating additionally available features to improve the torque estimation performance. Below, we summarize our findings from the above results: First, in addition to EMGs, using other motion-body features is very useful if we estimate the joint torque from other users’ data. Second, a simple linear model may not be sufficient to represent a novel user’s joint torque from other users’ data, even with the motion-body features. Third, in other words, a memory-based approach such as our method can show strong generalization performance with the motion-body features.

Fig. 10 shows representative examples of the nearest neighbor users and movement conditions when the joint torques of a novel subject are estimated with our approach using “EMGs only,” “EMGs and joint angles,” and all motion-body features under a motion condition with no-load and slow-speed movement. We found that the selected nearest user and motion condition to the novel subject varied during the multijoint movement under the three different feature conditions, and this trend was observed

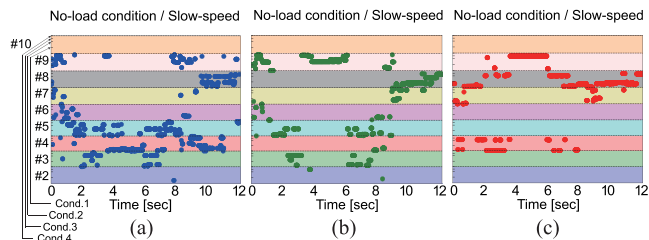


Fig. 10. Representative examples of nearest neighbor search in database when joint torques of subject #1 are estimated as novel user under a motion condition: No-load and slow-speed condition. Horizontal axis shows motion time and vertical axis shows all time-series data points of single-joint motion in four conditions of remaining nine users in database. (a) Nearest neighbor users calculated by EMGs only. (b) EMGs and joint angles. (c) All motion-body features.

in all other subjects and conditions. Regarding the joint torque estimation in this study, the selected nearest neighbor data by using all-motion body features seem to be relatively consistent against the other two. The body weight and the link length features are constant during the movement, and these features appear to stabilize the selection of the nearest neighbor data.

D. Online-Realtime Robot Control

In order to evaluate the feasibility of our proposed approach as a myoelectric interface for controlling external devices, we used our upper limb exoskeleton robot (see Fig. 5) with a mannequin arm. The total weight of the exoskeleton robot and the mannequin arm was close to the upper arm weight of a subject who conducted the robot control experiment. In this actual robot experiment, the number of neighboring data k in (6) and the time window for deriving the EMG vector l in (2) were set to $k = 1000$ and $l = 80$, respectively. We derived these values by averaging the metaparameters selected through the joint torque estimation processes in Section V-A (see also Appendix A).

The shoulder and elbow joints of the exoskeleton robot with its mannequin arm were controlled by the estimated torques using our collaborative filtering method under the *no-load* and *load* conditions. In the *load* condition, a 1-kg weight was attached to the tip of the mannequin. Fig. 11(a) shows the generated motion of the robot under the *no-load* condition, and Fig. 11(b) shows that under the *load* condition. The exoskeleton robot with a mannequin arm was successfully controlled using the proposed myoelectric interface in the two different load conditions.

To validate the joint angle trajectories generated by the estimated joint torques, we evaluated the correlation between the joint angles observed from the users’ actual motion and the joint angle trajectories of the robot. Since we used torque control and the physical properties of the robot with the attached mannequin arm are not equivalent to that of the human user, the movement amplitudes of the robot and the user can be different. Therefore, we evaluated the correlation rather than the joint angle differences. As a result, the average correlation over shoulder and elbow movements with the *no-load* and *load* conditions was 0.9. This high correlation indicates that our collaborative filtering method can properly estimate the joint torques in an

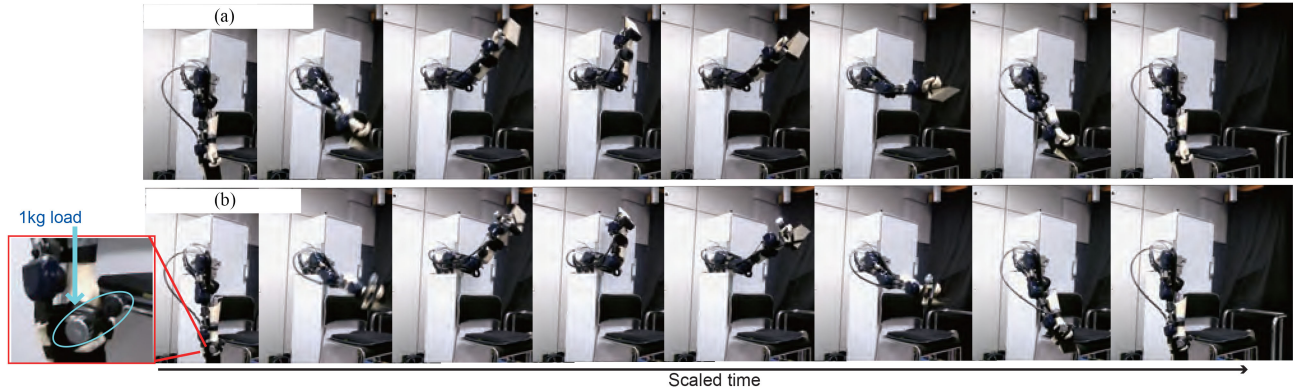


Fig. 11. Control performances of exoskeleton robot with a mannequin arm's upper limb attached. (a) No-load condition. (b) 1-kg load condition. The robot could be successfully controlled using the joint torques estimated by the proposed collaborative filtering approach.

online/real-time manner to generate the intended joint angle movements of the user.

VI. DISCUSSION

In this study, we introduced the concept of a collaborative filtering approach to estimate the joint torque of a novel user by exploiting the preidentified relationships between motion-body features, including EMG signals, and the joint torques of other users. In the evaluation, the joint torque estimation accuracy of our proposed approach outperformed the following two baseline methods.

- 1) *Linear-own*, where the parameters of the linear model were calibrated for each novel user from his/her own training data.
- 2) *Linear-others*, where the parameters of the linear model were calibrated with other user's data in which the novel user's data were not included.

In addition, we found that the proposed approach could successfully control an actual upper limb exoskeleton robot with a mannequin arm attached to it. From these results, our approach showed a strong potential to construct an EMG-based robot interface without the need for a time-consuming calibration process by using the data of other users.

Generally, EMG-based robot control faces the difficulty of electrode placement. Among different users, it is not clear how we should even define the corresponding electrode positions. Therefore, the best we can do is to place electrodes at similar positions based on biomechanical knowledge. However, even with this difficulty, the proposed method works well, possibly because it relies on the similarity between body-motion features rather than electrode placement. In addition, the proposed approach also requires the acquisition of MVC for first-time users, and the necessity of this identification process can be considered a limitation of our method, although MVC can be very easily detected.

The results of Fig. 8 indicate that we can possibly further improve the joint torque estimation performance if we additionally include relevant motion-body feature elements such as upper limb circumference [35]. In addition, since EMG measurement is known to be affected by subcutaneous fat [36], which can be

easily measured, it would be an interesting future study to also incorporate that information in the motion-body feature.

We used a camera-based motion capture system to measure the joint angles. This could also be considered a limitation of our approach when it is used in outdoor environments. As a possible solution, we could attempt to use an inertial measurement unit (IMU)-based motion capture system, as we previously used in a study on a rehabilitation robot [37]. Recently, a wearable IMU sensor system has become commercially available (e.g., Xenoma Inc.), and it could possibly be used for real-life applications.

In this study, the motion speed was set within a safe range for the experiments. However, these motions seem to be relatively slow compared to our daily life movements [38]. We will investigate how our approach works in a faster movement range in our future study.

We used low-pass filtering with a cutoff of 8 Hz. By following suggestions from the previous literature, we also tried other cutoff frequencies such as 4 Hz [39] and 6 Hz [40]. As a result, however, we did not find any significant difference in the joint torque estimation performance.

VII. CONCLUSION

In this study, we proposed a myoelectric interface based on the idea of collaborative filtering to achieve plug-and-play EMG-based robot control. In our approach, by using the extracted relationships between joint torques and motion-body features from other users, a new user does not need to calibrate parameters of the myoelectric interface. Despite its simplicity, our proposed approach outperformed the standard linear regression method that requires a calibration process. We also showed that a torque estimation model that separately uses elbow and shoulder single-joint movements as training data could be generalized to estimate the joint torques of shoulder-elbow multijoint movements. Furthermore, we found that the required computation time to estimate the joint torques was short enough for our method to be applied to an online/real-time control system. However, the estimation time needed to find the similarity between the novel user's data and the existing data in the collaborative filtering can increase when the number of users' data in the database becomes

much larger. To cope with this issue, our future study will focus on using parallel computation to implement collaborative filtering algorithms [41], [42].

Although we showed that our approach could estimate the joint torque even under conditions with additional load, the sudden occurrence of external forces has not been explicitly taken into account. For example, physical contact between the user and an object may lead to a sudden change of muscle activity and an unexpected movement of the robot. To cope with this type of situation, as a future study, we will consider combining the proposed collaborative filtering with an anomaly detection method [6] to safely derive joint torques.

Since our method opens the door to using other users' data to construct an EMG-based robot interface, we will attempt to collect a wider variety of motion-body data with the goal of managing versatile tasks.

APPENDIX

A. Setting Metaparameters

To determine the metaparameters of our joint torque estimation method, such as the number of neighboring data k of k -NN in (6) and the window size l to derive the EMG vector in (2), we adopted a nested cross-validation method. Concretely, in this study, we conducted experiments with ten subjects. Then, one of the ten subjects was considered a novel user and the selected subject's data were not used as training data. We then performed fourfold cross validation among the remaining nine subjects to determine the metaparameters. To find the number of neighboring data k , we set the search region from 100 to 3000 with a step size of 100. For online/real-time control, $k = 3000$ was the maximum number in our computational environment. To find the window size l , we set the search region from 10 to 200 with a step size of 10. By considering the time delay from EMG signal detection to the occurrence of muscle tension [8], [27], we set the upper bound of the search region to $l = 200$. We then conducted grid search with the above regions and step sizes in the cross-validation framework. For the number of neighboring data k , we found that $k = 1000$ was selected for 7 out of 10 subjects and the average was also $k = 1000$. This result indicates that we can find an appropriate metaparameter for k -NN by using a subset of data in a database and then use that parameter for the novel user. Note that the number of data points in our database was 180 000 ($= 9$ subjects $\times 2$ load conditions $\times 4$ motions per subject $\times 2500$ data points acquired from the slow- (12 s) and medium-speed (8 s) motions measured at the frequency of the 125-Hz sampling rate). Therefore, the frequently selected neighboring data size $k = 1000$ was much smaller than the entire set of data points in the database.

B. Linear Myoelectric Interface Model

We compared the proposed collaborative filtering approach with the standard linear regression models, *linear-own* and *linear-other*. Each model used different datasets but adopted the same linear conversion formula

$$\boldsymbol{\tau}(t) = \mathbf{K}\mathbf{u}^\top(t) \quad (7)$$

where $\boldsymbol{\tau}(t) = [\tau^1(t), \tau^2(t)]^\top$ is the estimated shoulder and elbow joint torques and $\mathbf{u}(t)$ is the normalized motion-body feature as introduced in Section III-A. We used the conventional least-squares algorithm to derive the parameter matrix \mathbf{K} .

REFERENCES

- [1] K. Ha, H. Varol, and M. Goldfarb, "Volitional control of a prosthetic knee using surface electromyography," *IEEE Trans. Biomed. Eng.*, vol. 58, no. 1, pp. 144–151, Jan 2011.
- [2] A. M. Dollar and H. Herr, "Lower extremity exoskeletons and active orthoses: Challenges and state-of-the-art," *IEEE Trans. Robot.*, vol. 24, no. 1, pp. 144–158, Feb. 2008.
- [3] M. A. Oskoei and H. Hu, "Support vector machine-based classification scheme for myoelectric control applied to upper limb," *IEEE Trans. Biomed. Eng.*, vol. 55, no. 8, pp. 1956–1965, Aug. 2008.
- [4] D. Zhang, X. Zhao, J. Han, and Y. Zhao, "A comparative study on PCA and LDA based EMG pattern recognition for anthropomorphic robotic hand," in *Proc. IEEE Int. Conf. Robot. Automat.*, May 2014, pp. 4850–4855.
- [5] T. Lenzi, S. De Rossi, N. Vitiello, and M. Carrozza, "Intention-based EMG control for powered exoskeletons," *IEEE Trans. Biomed. Eng.*, vol. 59, no. 8, pp. 2180–2190, May 2012.
- [6] J. Furukawa, T. Noda, T. Teramae, and J. Morimoto, "Human movement modeling to detect biosignal sensor failures for myoelectric assistive robot control," *IEEE Trans. Robot.*, vol. 33, no. 4, pp. 846–857, Aug. 2017.
- [7] K. Kiguchi and Y. Hayashi, "An EMG-based control for an upper-limb power-assist exoskeleton robot," *IEEE Trans. Syst., Man, Cybern., B, Cybern.*, vol. 42, no. 4, pp. 1064–1071, Aug. 2012.
- [8] Y. Koike and M. Kawato, "Estimation of dynamic joint torques and trajectory formation from surface electromyography signals using a neural network model," *Biol. Cybern.*, vol. 73, no. 4, pp. 291–300, Sep. 1995.
- [9] L. Pan, D. L. Crouch, and H. Huang, "Myoelectric control based on a generic musculoskeletal model: Toward a multi-user neural-machine interface," *IEEE Trans. Neural Syst. Rehabil. Eng.*, vol. 26, no. 7, pp. 1435–1442, Jul. 2018.
- [10] F. Cordella *et al.*, "Literature review on needs of upper limb prosthesis users," *Front. Neurosci.*, vol. 10, pp. 1–14, May 2016.
- [11] O. Mohamed, J. Perry, and H. Hislop, "Relationship between wire EMG activity, muscle length, and torque of the hamstrings," *Clin. Biomech.*, vol. 17, no. 8, pp. 569–579, Oct. 2002.
- [12] N. U. Ahamed, N. Ahamed, M. Alqahtani, O. Altwijiri, R. Ahmad, and K. Sundaraj, "Investigation of the EMG-time relationship of the biceps Brachii muscle during contractions," *J. Phys. Ther. Sci.*, vol. 27, no. 1, pp. 39–40, Jan. 2015.
- [13] H. Li, G. Zhao, Y. Zhou, X. Chen, Z. Ji, and L. Wang, "Relationship of EMG/SMG features and muscle strength level: An exploratory study on tibialis anterior muscles during plantar-flexion among hemiplegia patients," *Biomed. Eng. OnLine*, vol. 13, no. 1, pp. 1–15, Jan. 2014.
- [14] F. Ricci, L. Rokach, and B. Shapira, *Introduction to Recommender Systems Handbook*. Boston, MA, USA: Springer, 2011.
- [15] J. Furukawa, A. Takai, and J. Morimoto, "Database-driven approach for biosignal-based robot control with collaborative filtering," in *Proc. IEEE-RAS 17th Int. Conf. Humanoid Robot.*, 2017, pp. 606–611.
- [16] F. Orabona, C. Castellini, B. Caputo, A. E. Fiorilla, and G. Sandini, "Model adaptation with least-squares SVM for adaptive hand prosthetics," in *Proc. IEEE Int. Conf. Robot. Automat.*, 2009, pp. 2897–2903.
- [17] A. Xiong, X. Zhao, J. Han, G. Liu, and Q. Ding, "An user-independent gesture recognition method based on sEMG decomposition," in *Proc. IEEE/RSJ Int. Conf. Intell. Robots Syst.*, 2015, pp. 4185–4190.
- [18] T. Matsubara and J. Morimoto, "Bilinear modeling of EMG signals to extract user-independent features for multiuser myoelectric interface," *IEEE Trans. Biomed. Eng.*, vol. 60, no. 8, pp. 2205–2213, Aug. 2013.
- [19] C. Fleischer and G. Hommel, "A human-exoskeleton interface utilizing electromyography," *IEEE Trans. Robot.*, vol. 24, no. 4, pp. 872–882, Aug. 2008.
- [20] P. K. Artemiadis and K. J. Kyriakopoulos, "EMG-based control of a robot arm using low-dimensional embeddings," *IEEE Trans. Robot.*, vol. 26, no. 2, pp. 393–398, Apr. 2010.
- [21] J. M. Hahne *et al.*, "Linear and nonlinear regression techniques for simultaneous myoelectric control," *IEEE Trans. Neural Syst. Rehabil. Eng.*, vol. 22, no. 2, pp. 269–279, Mar. 2014.

- [22] L. H. Smith, T. A. Kuiken, and L. J. Hargrove, "Evaluation of linear regression simultaneous myoelectric control using intramuscular EMG," *IEEE Trans. Biomed. Eng.*, vol. 63, no. 4, pp. 737–746, Apr. 2016.
- [23] S. Sorawit, K. Yeongdae, T. Atsushi, Y. Natsue, and K. Yasuharu, "Finger angle estimation from array EMG system using linear regression model with independent component analysis," *Front. Neurobot.*, vol. 13, pp. 1–12, Sep. 2019.
- [24] A. Hill, "The heat of shortening and the dynamic constants of muscle," *Proc. Roy. Soc. London B., Biol. Sci.*, vol. 126, no. 843, pp. 136–195, Oct. 1938.
- [25] H. Hatze, "A myocybernetic control model of skeletal muscle," *Biol. Cybern.*, vol. 25, pp. 103–119, Jan. 1977.
- [26] F. Romero and F. J. Alonso, "A comparison among different Hill-type contraction dynamics formulations for muscle force estimation," *Mech. Sci.*, vol. 7, no. 1, pp. 19–29, Jan. 2016.
- [27] D. A. Winter, *Biomechanics and Motor Control of Human Movement*. Hoboken, NJ, USA: Wiley, 2009.
- [28] X. Su and T. M. Khoshgoftaar, "A survey of collaborative filtering techniques," *Adv. Artif. Intell.*, vol. 2009, Oct. 2009, Art. no. 421425.
- [29] N. S. Altman, "An introduction to kernel and nearest-neighbor non-parametric regression," *Amer. Statistician*, vol. 46, no. 3, pp. 175–185, Aug. 1992.
- [30] M. Murugappan, "Electromyogram signal based human emotion classification using KNN and LDA," in *Proc. IEEE Int. Conf. Syst. Eng. Technol.*, Jun. 2011, pp. 106–110.
- [31] E. Todorov, "Probabilistic inference of multijoint movements, skeletal parameters and marker attachments from diverse motion capture data," *IEEE Trans. Biomed. Eng.*, vol. 54, no. 11, pp. 1927–1939, Nov. 2007.
- [32] T. Noda, T. Teramae, B. Ugurlu, and J. Morimoto, "Development of an upper limb exoskeleton powered via pneumatic electric hybrid actuators with bowden cable," in *Proc. IEEE/RSJ Int. Conf. Intell. Robots Syst.*, Sep. 2014, pp. 3573–3578.
- [33] C. Fleischer, C. Reinicke, and G. Hommel, "Predicting the intended motion with EMG signals for an exoskeleton orthosis controller," in *Proc. IEEE/RSJ Int. Conf. Intell. Robots Syst.*, Aug. 2005, pp. 2029–2034.
- [34] J. Furukawa, T. Noda, T. Teramae, and J. Morimoto, "An EMG-driven weight support system with pneumatic artificial muscles," *IEEE Syst. J.*, vol. 10, no. 3, pp. 1026–1034, Sep. 2016.
- [35] X. Wang, X. Tao, and R. C. H. So, "A bio-mechanical model for elbow isokinetic and isotonic flexions," *Sci. Rep.*, vol. 7, no. 1, pp. 1–10, Aug. 2017.
- [36] T. A. Kuiken, M. M. Lowery, and N. S. Stoykov, "The effect of subcutaneous fat on myoelectric signal amplitude and cross-talk," *Prosthetics Orthotics Int.*, vol. 27, no. 1, pp. 48–54, Apr. 2003.
- [37] T. Teramae, T. Matsubara, T. Noda, and J. Morimoto, "Quaternion-based trajectory optimization of human postures for inducing target muscle activation patterns," *IEEE Robot. Automat. Lett.*, vol. 5, no. 4, pp. 6607–6614, Oct. 2020.
- [38] A. W. Wiegner and M. M. Wierzbicka, "Kinematic models and human elbow flexion movements: Quantitative analysis," *Exp. Brain Res.*, vol. 88, no. 3, pp. 665–673, 1992.
- [39] Y. Li, W. Chen, H. Yang, J. Li, and N. Zheng, "Joint torque closed-loop estimation using NARX neural network based on sEMG signals," *IEEE Access*, vol. 8, pp. 213636–213646, 2020.
- [40] D. G. Lloyd and T. F. Besier, "An EMG-driven musculoskeletal model to estimate muscle forces and knee joint moments in vivo," *J. Biomech.*, vol. 36, no. 6, pp. 765–776, 2003.
- [41] J. Maillo, I. Triguero, and F. Herrera, "A MapReduce-based k-nearest neighbor approach for big data classification," in *Proc. IEEE Int. Conf. Trust, Secur. Privacy Comput. Commun.*, Aug. 2015, vol. 2, pp. 167–172.
- [42] Y. Zhou, D. Wilkinson, R. Schreiber, and P. Rong, "Large-scale parallel collaborative filtering for the Netflix prize," in *Proc. Int. Conf. Algorithmic Aspects Inf. Manage.*, vol. 5034, Jun. 2008, pp. 337–348.



Jun-ichiro Furukawa (Member, IEEE) received the Ph.D. degree in engineering from Osaka University, Osaka, Japan in 2016.

From 2016 to 2020, he was a Researcher with the Department of Brain Robot Interface, ATR Computational Neuroscience Laboratories, Kyoto, Japan. He is currently a Research Scientist with the Man-Machine Collaboration Research Team, Guardian Robot Project, RIKEN Information R&D and Strategy Headquarters, Kyoto.



Shinya Chiyohara received the Master of Science degree from Osaka University, Osaka, Japan, in 2016.

He obtained a physical therapist license in 2007 and has provided care for people in a variety of settings, including hospitals, outpatient clinics, and home health agencies. He is currently an Intern with the Cognitive Neuroscience, ATR Cognitive Mechanisms Laboratories, Kyoto, Japan. His research interests include human motor control, interactions between cognition and motor control, and human–robot interaction.



Tatsuya Teramae received the Ph.D. degree in engineering from Tottori University, Tottori, Japan, in 2011.

He is currently a Researcher with the Department of Brain Robot Interface, ATR Computational Neuroscience Laboratories, Kyoto, Japan. His research interests include robot control and optimization in human-robot system.

Dr. Teramae is a Member of the Japan Neuroscience Society, the Society of Instrument and Control Engineers in Japan, and the Institute of Electrical

Engineers of Japan.



Asuka Takai received the Doctor of Engineering degree from Osaka Prefecture University, Sakai, Japan, in 2015.

She is currently a Researcher with the Department of Brain Robot Interface, ATR Computational Neuroscience Laboratories, Kyoto, Japan. Under the cross-appointment system, she also belongs to the Mechanical and Physical Engineering Course, Graduate School of Engineering, Osaka City University, Osaka, Japan. Her research interests include human movement assistive engineering and rehabilitation

and human–human and human–robot interaction.

Dr. Takai is a Member of the Japan Society of Mechanical Engineers and the Society of Biomechanisms Japan.



Jun Morimoto (Member, IEEE) received the Ph.D. degree in information science from the Nara Institute of Science and Technology, Nara, Japan, in 2001.

From 2001 to 2002, he was a Postdoctoral Fellow with the Robotics Institute, Carnegie Mellon University, Pittsburgh, PA, USA. He Joined Advanced Telecommunications Research Institute International (ATR) in 2002. He was also with JST, ICORP, from 2004 to 2009. He is currently a Professor with the School of Informatics, Kyoto University, Kyoto, Japan. He is also the Head of the Department of Brain

Robot Interface (BRI), ATR Computational Neuroscience Laboratories, Kyoto, and a Senior Visiting Scientist with Man–Machine Collaboration Research Team, Guardian Robot Project, RIKEN, Kyoto.